electronics

Article

Adaptive Handover Decision Using Fuzzy Logic for 5G Ultra-Dense Networks

Wen-Shyang Hwang [1], Teng-Yu Cheng [1], Yan-Jing Wu [2,*] and Ming-Hua Cheng [3]

1 Department of Electrical Engineering, National Kaohsiung University of Science and Technology, Kaohsiung 807618, Taiwan
2 Department of Information Technology and Communication, Shih Chien University, Kaohsiung Campus, Kaohsiung 845050, Taiwan
3 Department of Digital Media Design, Tzu-Hui Institute of Technology, Pingtung 926001, Taiwan
* Correspondence: yanjing@g2.usc.edu.tw

Abstract: With the explosive increase in traffic volume in fifth-generation (5G) mobile wireless networks, an ultra-dense network (UDN) architecture, composed of highly concentrated millimeter-wave base stations within the fourth-generation (4G) system, has been developed. User equipment (UE) may encounter more frequent handover opportunities when moving in a UDN. Conventional handover schemes are too simple to adapt to the diverse handover scenarios encountered in 5G UDNs because they consider only UE signal strength. Unnecessary handovers aggravate the ping-pong effect and degrade the quality of service of cellular networks. Fuzzy logic (FL) is considered the best technique to unravel the handover problem in a high-density scenario of small cells for 4G/5G networks. In this paper, we propose an FL-based handover scheme to dynamically adjust the values of two handover parameters, namely handover margin (HOM) and time to trigger (TTT), with respect to each UE. The proposed scheme, abbreviated as FLDHDT, has dynamic adjustment of TTT in addition to HOM by using the signal to interference plus noise ratio and horizontal moving speed of the UE as inputs to the FL controller. To demonstrate the effectiveness and superiority of FLDHDT, we perform simulations using the well-known ns-3 simulator. The performance measures include the number of handovers, overall system throughput, and ping-pong ratio. The simulation results demonstrate that FLDHDT improves the handover performance of 5G UDNs in terms of the number of handovers, ping-pong ratio, and overall system throughput compared to a conventional handover scheme, namely Event A3, and an FL-based handover scheme with dynamic adjustment of only HOM.

Keywords: UDN; handover; HOM; TTT; fuzzy logic

Citation: Hwang, W.-S.; Cheng, T.-Y.; Wu, Y.-J.; Cheng, M.-H. Adaptive Handover Decision Using Fuzzy Logic for 5G Ultra-Dense Networks. *Electronics* **2022**, *11*, 3278. https://doi.org/10.3390/electronics11203278

Academic Editors: Konstantinos Ntontin and Alexandros-Apostolos Boulogeorgos

Received: 11 September 2022
Accepted: 9 October 2022
Published: 12 October 2022

1. Introduction

Since 2019, telecommunication companies have started to deploy fifth-generation (5G) mobile communication networks to replace the existing fourth-generation (4G) communication networks. By 2025, the number of pieces of user equipment (UE) worldwide is expected to grow to 1.7 billion [1]. Ericsson Telecommunications predicts that the global mobile data traffic volume will reach 370 EB monthly by 2027, which is 4.4 times the monthly volume of 80 EB at the end of 2021. 5G systems are expected to carry 62% of mobile data traffic by 2027 [2]. The 5G network architecture is cellular, and the service area is divided into numerous small cells. All the UE in each cell transmit radio waves to communicate with the base station (BS) that covers the cell. The BSs are wired through high-bandwidth fiber optics to the public switched telephone network and to routers for Internet access. The millimeter-wave (mmWave) frequency band and multiple in, multiple out (MIMO) technology are used to increase network capacity, and therefore, 5G may be able to support up to one million mobile devices per square kilometer, which is 10 times the number of mobile devices supported by 4G networks over the same area. Identical to the existing cellular networks, handover occurs when a device moves from one cell to another cell. On the other hand, joint beamforming design and optimization, security, and energy efficiency of mmWave and MIMO are continuously investigated for satellite communications [3–5].

With the aforementioned explosive growth in traffic volume, cellular network fragmentation and densification have emerged as the most effective technologies for increasing network capacity and improving user experience. In recent years, ultra-dense networks (UDNs) have been developed as a crucial solution to support capacity densities of up to 10 Mbps/m^2 in 5G networks. However, the propagation distance of millimeter radio waves is up to 300 m. Therefore, smaller BSs must inevitably be set up at intervals of a few hundred meters to extend the service coverage, resulting in a UDN-like architecture. In terms of cell coverage, BSs are classified as macro-, micro-, femto-, and picocells depending on their cell radii. Among them, micro-, femto-, and picocells are considered small cells. Several definitions of UDNs have been proposed in terms of cell quantity. In [6,7], a UDN is defined as a cellular network with a BS density that may be equal to or greater than the user density, which is suitable for describing a scenario in which user traffic increases but the number of users does not. Alternatively, a UDN is defined as a cellular network that offers coverage of a few meters between any two BSs [8]. In addition, a UDN is a cellular network in which the number of BSs increases linearly as the demand for network capacity increases [9].

As depicted in Figure 1, a 5G UDN is typically a heterogeneous network composed of dense mmWave BSs and traditional 4G BSs. Although 5G UDNs can significantly improve network capacity, they are fraught with multiple problems. For instance, inter-cell interference is more severe, optimal utilization of radio resources is more complex, and load distribution among BSs is more unbalanced. Specifically, the UE moving within a UDN are likely to encounter more frequent handover opportunities that lead to handover-related problems, such as premature/late handover decisions and the ping-pong effect. Handover execution at an inappropriate time may interrupt data transmission links. The ping-pong effect refers to the back-and-forth handover phenomenon between two BSs that is caused by unstable signal strength resulting from the movement of UE close to the edge of a BS's coverage. As summarized in Table 1, the 3rd Generation Partnership Project (3GPP) defines the trigger scenarios of handover decision for cellular networks [10]. A-series events correspond to horizontal handovers, that is, handover between two BSs based on the same radio access technology (RAT), whereas B-series events correspond to vertical handovers, that is, handover between two BSs based on different RATs.

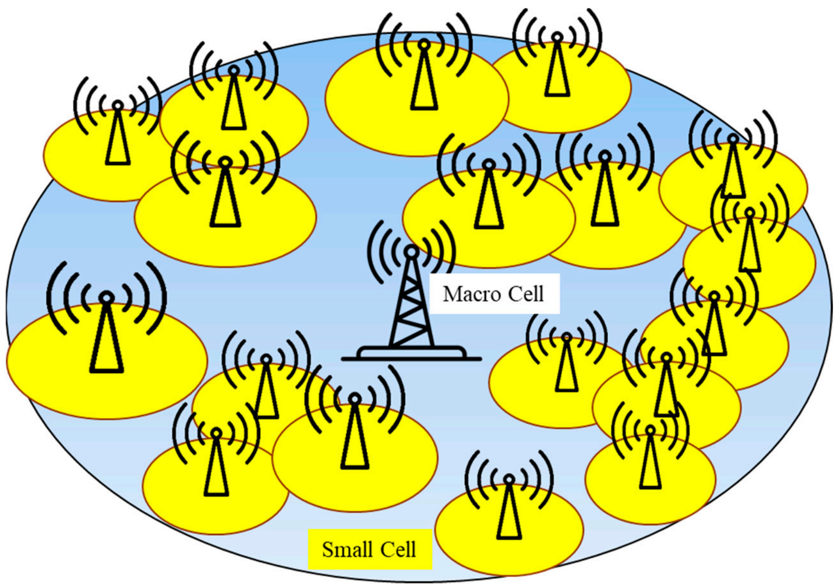

Figure 1. 5G UDN architecture.

Table 1. Measurement report yriggering.

Event	Trigger Scenario
A1	Serving is better than the threshold
A2	Serving is worse than the threshold
A3	Neighbor is offset better than the serving cell
A4	Neighbor is better than the threshold
A5	Serving is worse than threshold_1, and neighbor is better than threshold_2
A6	Neighbor is offset better than the secondary serving cell
B1	Inter-RAT neighbor is better than the threshold
B2	Serving is worse than threshold_1, and inter-RAT neighbor is better than threshold_2

Starting with 4G networks, Event A3 has been implemented for handover triggering. 5G networks also use Event A3 for performing handovers. As depicted in Figure 2, when the signal strength of the neighbor BS is greater than that of the serving BS plus a threshold value and an offset, which is designated as the handover margin (HOM), handover is performed after waiting for a time-to-trigger (TTT) duration. HOM and TTT are used to make handover decisions to avoid the ping-pong effect and alleviate the control burden of BSs. The 5G era is characterized by larger bandwidth, lower latency, and smaller cell coverage. In this context, mmWave technology can support high-density BS deployment for hotspots, perform high-precision positioning of UE, and facilitate equipment integration. Therefore, it is beneficial to promote the miniaturization of base stations and user terminals.

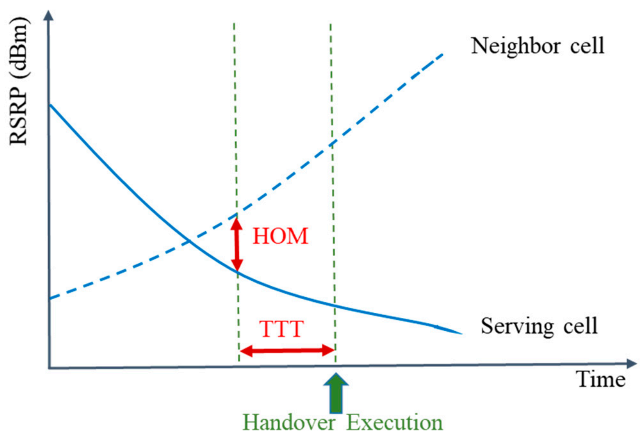

Figure 2. Event A3 handover procedure.

The UE moving within a 5G UDN may encounter more frequent handover opportunities because the cell coverage of each small BS is not as wide as that of 4G BSs, and handover scenarios in 5G UDNs appear to be more complex. In 4G network environments, handovers are only performed at the cell edge of a BS, and there are fewer target BS candidates. Consequently, the use of Event A3 for making handover decisions can lead to good performance. However, the use of Event A3 with fixed HOM and TTT for making handover decisions is not reliable for 5G UDNs, because UE may frequently move forward into a certain area where the cell coverage of multiple BSs overlaps. Moreover, individual handover parameter values are essential for different UEs to adapt to diverse handover scenarios. For example, when the signal strength of the serving BS is good, a high HOM can prevent unnecessary handovers or the ping-pong effect. In addition, for UE moving at a high speed, small HOM and TTT can lead to more successful handovers in time.

Fuzzy logic (FL) [11,12] is a well-known method for translating the domain knowledge of human experts into a rule base and for experts to formalize uncertainty. FL is considered the best technique to unravel the handover problem in a high-density scenario of small cells for 4G/5G networks [13]. Recently, numerous FL-based handover schemes, which are elaborated in Section 2, have been proposed for making handover decisions more accurately in time. To alleviate unnecessary handovers and avoid a severe ping-pong effect in 5G UDNs, we propose an FL-based handover algorithm with dynamic HOM and dynamic TTT (abbreviated as FLDHDT) by using the signal to interference plus noise ratio (SINR) and horizontal moving speed of UE as inputs to the FL controller. We performed simulations using the well-known ns-3 simulator to demonstrate the effectiveness and superiority of the proposed FLDHDT. The performance measures include the number of handovers, overall system throughput, and ping-pong ratio.

The remainder of this paper is organized as follows. Section 2 explores the related literature. Section 3 describes the operating procedures of the proposed FLDHDT. Section 4 analyzes and compares the simulation results. Finally, our concluding remarks and an outline of future works are summarized in Section 5.

2. Related Works

There are two types of handover, namely hard and soft. The transmission channel inevitably has a short gap in hard handover because the channel connected to the serving BS is released before it is connected to the target BS. The advantage of hard handover is that only one channel is used for a UE at any time, and its disadvantage is that the transmission channel may be temporarily interrupted or even abnormally terminated if the handover fails. Soft handover retains the channel connected to the serving BS and uses the channel connected to the target BS in parallel for a certain period. The advantage of soft handover is that the connection link to the serving BS is disconnected after a reliable connection link to the target BS is established, whereas its disadvantage is that the system capacity decreases because multiple channels are occupied during a handover procedure. Because the cost of hard handover is considerably lower than that of soft handover and the interruption gap of hard handover is acceptable for maintaining the desired transmission quality, all mobile wireless networks implemented have used hard handover. Accordingly, most of the recent works on handover decisions have investigated hard handover.

As mentioned in Section 1, Event A3 is used as the trigger scenario to make handover decisions in 4G/5G networks. Two handover parameters, HOM and TTT, are used to decide when to execute handover from the serving cell to the target cell. Once the reference signal receiving power (RSRP) of the target BS is higher than that of the serving BS plus HOM for the duration of TTT, handover execution is performed. One of the drawbacks of using Event A3 is that HOM and TTT are fixed for each UE. Moreover, only the reported RSRP is used as the input in the handover decision procedure without considering other factors, such as UE speed, distance between BS and UE, and BS loading.

The authors of [14,15] described software-defined networking (SDN)-based handover decisions for 5G UDNs. Their SDNs are responsible for a global view of network topology and centralized control to facilitate seamless handovers in cellular/IEEE 802.11p hybrid networks and to shorten the handover execution time, respectively. On the other hand, numerous authors applied artificial intelligence techniques to handover management in 5G [16,17]. Yajnanarayana et al. [18] proposed a novel method for maximizing the long-term link-beam RSRP after handover by using reinforcement learning for three pre-defined deployments of 5G cellular architecture. Zhao et al. [19] presented a model for predicting user trajectory by combining convolutional neural networks and long short-term memory to identify the traffic demands of all BSs in advance to improve network resource utilization and user experience in 5G UDNs. Recently, many researchers [20–25] have used FL to design adaptive handover decision schemes for 5G. The authors of [20,21] proposed FL-based handover algorithms to dynamically adjust only HOM. The difference between the two algorithms proposed in these studies is that the former uses only SINR as an input to the FL controller, while the latter uses UE speed and SINR. The authors of [22,23] developed vertical handover decision algorithms considering various RATs by taking into account SINR, bandwidth, cost, or UE velocity. The output of their FL controller is the most suitable RAT for accessing the Internet, aiming to reduce the number of interruptions and handoff processing delays. Banna et al. [24] presented a fast adaptive handover algorithm by using

FL in 5G cellular networks only for high-speed trains, which operate at speeds equal to or higher than 400 km/h. Their algorithm comprises two phases. The first is selection of the target BS in advance according to the trajectory of the train. The other is to dynamically adjust the TTT in the range of [0, 250 ms] by using cell size and train speed as inputs to the FL controller. Saddam Alraih et al. [25] proposed a robust handover optimization technique with FL controller (RHOT-FLC). The proposed RHOT-FLC aimed to automatically configure both HOM and TTT by exploiting the information on RSRP, reference signal received quality, and UE velocity as input factors. Additionally, the inference rules were determined based on the evaluation conducted on each rule and all of the performance metrics to achieve mobility robustness optimization at the cost of computation loads and times.

Because FL can provide relatively reliable outcomes with lower computational costs and shorter times, it has been widely applied in many fields, including for making handover decisions in mobile cellular networks. The correctness of the inference engine of FL depends on the choice of input factors, membership functions (MFs), rule base size, and others. The main contribution of our work is the proposed adaptive handover decision algorithm that uses FL to effectively alleviate unnecessary handovers and reduce the ping-pong effect in 5G UDNs by dynamically adjusting TTT in addition to HOM. The inputs to the FL controller are only the signal strength and horizontal moving speed of user devices, and the outputs are the HOM and TTT values for each piece of UE.

3. Proposed FLDHDT

3.1. System Architecture

The 5G UDN we consider in this paper is heterogeneously composed of 4G BSs (i.e., evolved NodeB, eNB) and 5G BSs (i.e., next-generation NodeB, gNB) overlaid on the coverage of 4G BSs. Option 3 of the non-standalone (NSA) networking mode is used, in which the control functions rely on the control plane of the existing 4G networks while the 5G network focuses on the user plane [10]. The NSA networking mode—specifically the coexistence of 5G and 4G—is apt for accelerating the commercialization of 5G. By using Option 3 of the NSA networking mode, UEs are configured with dual connectivity technology, meaning that they are connected to both eNB and gNB. Control signalling is transmitted from the eNB to the evolved packet core (EPC) network of 4G, and user data are preferentially transmitted from the gNB to the EPC through the eNB, as depicted in Figure 3.

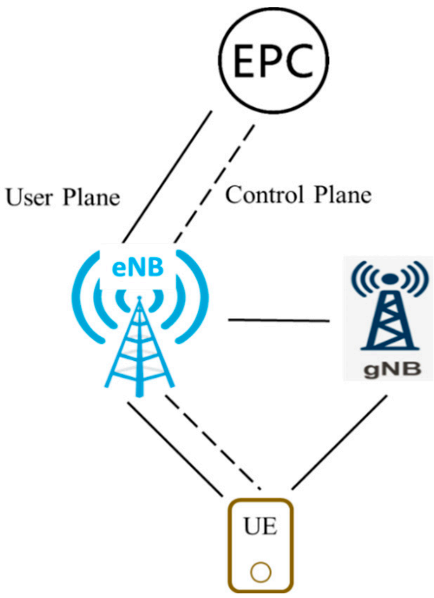

Figure 3. Option 3 of the NSA networking mode.

3.2. Adaptive Handover Decision Using Fuzzy Logic

In this study, we propose an FL-based handover algorithm with dynamic HOM and dynamic TTT (abbreviated as FLDHDT) for 5G UDNs. The proposed FLDHDT can configure the appropriate handover parameters for UEs on the basis of their individual inputs. An FL controller is used to dynamically adjust both the HOM and TTT. The inputs to the FL controller are the signal strength and horizontal moving speed of user devices, and the outputs are the HOM and TTT values of each piece of UE. FLDHDT consists of three stages: data pre-processing, inference using FL, and handover decision.

3.2.1. Data Pre-Processing

The serving BS can request relevant information from the UE through measurement reports, such as the signal strengths of the UE to all neighboring BSs, geometrical location of the UE, and moving speed of the UE. FLDHDT uses the SINR and horizontal moving speed of the UE as inputs to the FL controller. The signal strength of the UE is always the most important input factor governing handover decision, such as the Event A3 defined in the 4G/5G standards. Moreover, the moving speed of the UE is a crucial input governing handover decision. In general, a lower HOM and shorter TTT are more suitable for relatively high-speed UE because high-speed UE has smaller processing time tolerances for the handover decision. Conversely, a higher HOM and longer TTT are more suitable for low-speed UE to avoid unnecessary handovers.

The cell coverage of a BS is similar to a circle or an ellipse. Thus, the horizontal scalar speed of the UE velocity vector indicates how fast the UE is moving away from the serving BS. As illustrated in Figure 4, $\vec{u}$ (in light blue) is obtained from the difference between the geometric locations of the UE and the serving BS, and $\vec{v}$ (in dark blue) denotes the velocity of the UE. Thus, we can obtain the angle, denoted by θ, between the two vectors, as expressed in Equation (1) and the horizontal moving speed of the UE (plotted by a red line segment) as $\vec{v}$ times cosθ. Notably, UE1 and UE2 have the same velocity and are at the same distance from the serving BS, but UE1 is moving away from the serving BS faster than UE2 because the horizontal speed of UE1 is higher.

$$\cos\theta = \frac{\vec{u}\cdot\vec{v}}{\left|\vec{u}\right|\cdot\left|\vec{v}\right|}, -90^{\circ} \leqq \theta \leqq 90^{\circ} \tag{1}$$

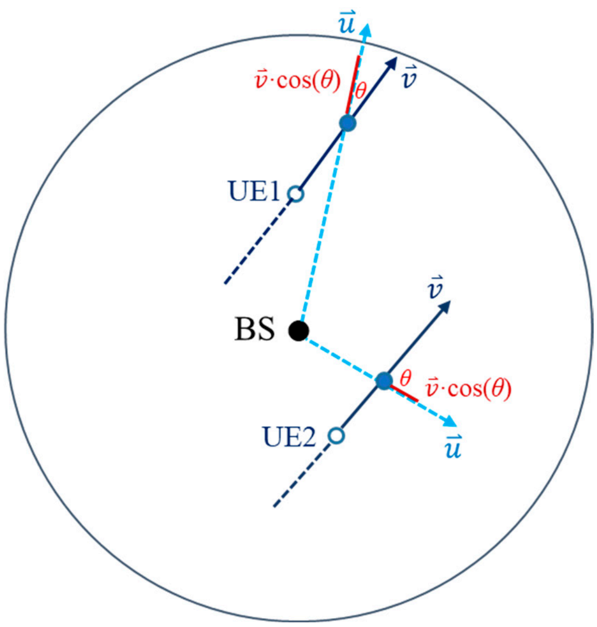

Figure 4. Illustration of the horizontal moving speed of UE.

3.2.2. Inference Using Fuzzy Logic

The general architecture of an FL controller comprises three components, namely a fuzzifier, rule base and inference engine, and defuzzifier [26]. As depicted in Figure 5, the inputs to the fuzzifier used in FLDHDT are the SINR and horizontal speed of the UE, and the outputs of the defuzzifier are the HOM and TTT values for the UE.

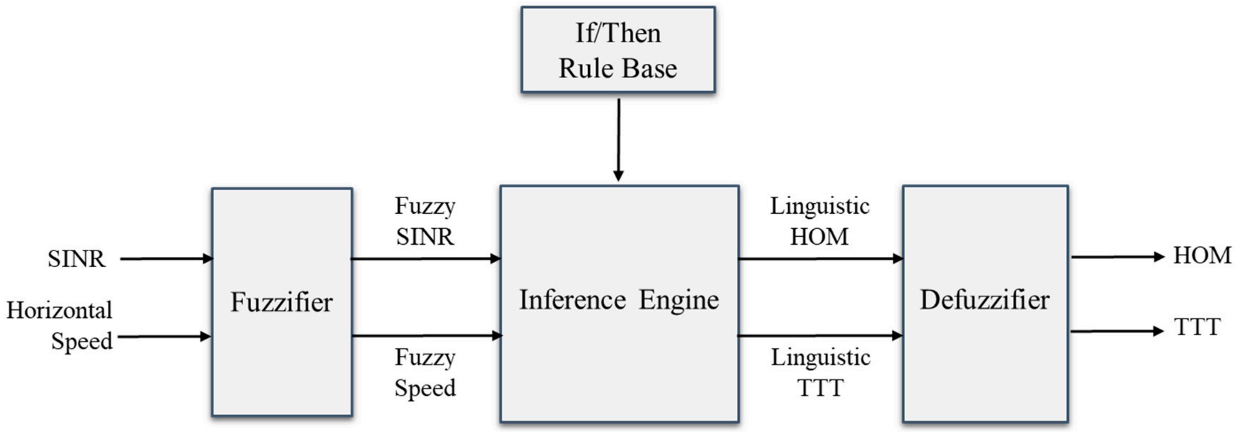

Figure 5. FL controller of FLDHDT.

A. Fuzzifier

The fuzzifier passes each crisp input through an MF to generate a corresponding fuzzy input. Each crisp input variable has a corresponding MF that operates independently of the other MFs. The most commonly used MFs are triangular MF, trapezoidal MF, bell MF, and Gaussian MF. However, the shape of the curve is usually not as important as the number and positions of the curves. Three to seven curves are usually suitable for transferring all possible input values [27]. The Cable Free Team at Wireless Excellence Limited provided a classification of signal strength [28], which is summarized in Table 2. By referring to Table 2, in FLDHDT, we used three triangular functions as the MF to divide the SINR range of [−10 dB, 30 dB] into four SINR-value-based intervals, namely bad, bad + mid_P, mid_P+good, and good, as depicted in Figure 6. The degree of the MF of the SINR is expressed as Equation (2), where P denotes the SINR of the UE. Similarly, three triangular functions are used in the MF to represent the horizontal speed of the UE. By considering scenarios that include pedestrians, bikes, vehicles, and local and express trains, with the exception of ultrafast vehicles such as high-speed trains, the range of horizontal speed was set as 0 to 20 m/s, and it was divided into four intervals, namely slow, slow+mid_V, mid_V+fast, and fast, as depicted in Figure 7. The degree of the MF of the UE horizontal speed is expressed as Equation (3), where V represents the horizontal speed of the UE.

Table 2. Signal strength indicator.

Signal Strength	RSRP (dBm)	RSRQ (dB)	SINR (dB)
Excellent	≧−80	≧−10	≧20
Good	−80~−90	−10~−15	13~20
Mid Cell	−90~−100	−15~−20	0~13
Cell Edge	≦−100	≦−20	≦0

$$(P) = \begin{cases} 1 * bad, \quad P \leq 0 \\ \frac{13-P}{13-0} * bad + \frac{P-0}{13-0} * mid\_P, \quad 0 < P \leq 13 \\ \frac{20-P}{20-13} * mid\_P + \frac{P-13}{20-13} * good, \quad 13 < P \leq 20 \\ 1 * good, \quad P > 20 \end{cases} \tag{2}$$

$$f(V)\begin{cases} \frac{6-V}{6-0} * slow, \;\; V \le 3 \\ max\left\{0,\, \frac{6-V}{6-0}\right\} * slow + \frac{V-3}{10-3} * mid\_V, \;\; 3 < V \le 10 \\ \frac{16-V}{16-10} * mid\_V + max\left\{0,\, \frac{V-13}{20-13}\right\} * fast, \;\; 10 < V \le 16 \\ \frac{V-13}{20-13} * fast, \;\; V > 16 \end{cases} \tag{3}$$

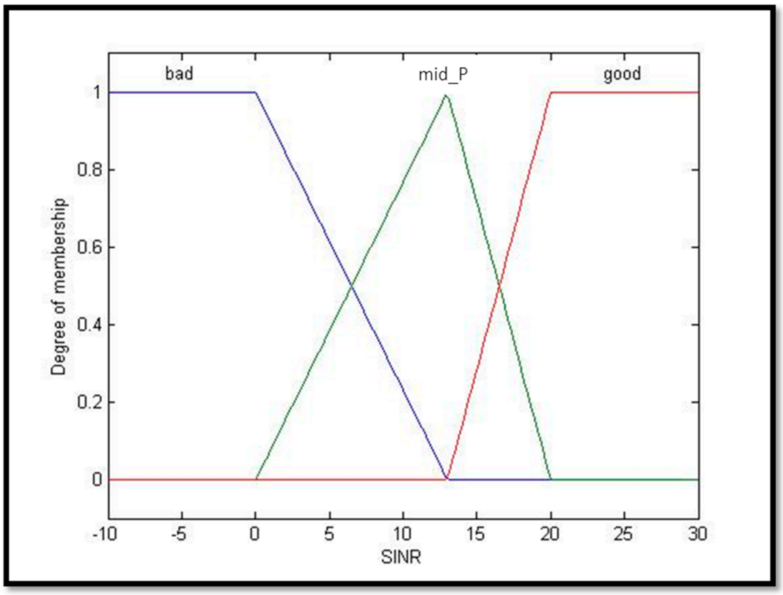

Figure 6. Membership function of SINR.

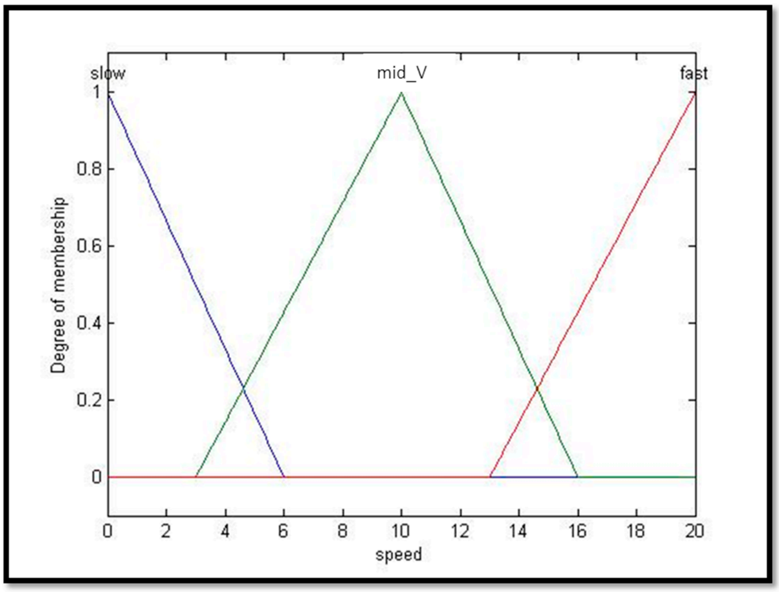

Figure 7. Membership function of horizontal speed.

B. Inference Engine and Rule Base

The fuzzifier maps a crisp input to a corresponding fuzzy input. Then, the inference engine generates linguistic outputs according to the rule base. Table 3 lists the rule base designed for FLDHDT. Because there are two groups of three fuzzy inputs, all possible fuzzy outputs are obtained using the AND operator, and nine rules are generated for either HOM or TTT. The HOM values are divided into three levels {A, B, C} with respect to the SINR intensity and subdivided into three levels {+, 0, −} with respect to the horizontal UE speed. Similarly, the TTT values are divided into three levels {A, B, C} with respect to the horizontal UE speed and subdivided into three levels {+, 0, −} with respect to the SINR of the UE.

Table 3. Rule base of inference engine.

In		Out	
SINR	**Speed**	**HOM**	**TTT**
bad	fast	C-	C-
bad	mid_V	C	B-
bad	slow	C+	A-
mid_P	fast	B-	C
mid_P	mid_V	B	B
mid_P	slow	B+	A
good	fast	A-	C+
good	mid_V	A	B+
good	slow	A+	A+

C. Defuzzifier

The defuzzifier transfers a linguistic input into a crisp output after the linguistic input is generated by the inference engine on the basis of the rule base. The center of gravity (CoG) method [29] is the most commonly used for defuzzification. The CoG method calculates the center point of all overlapping areas that are obtained from the fuzzy outputs for HOM (TTT) in the corresponding MF, as plotted in Figures 8 and 9 of FLDHDT. In Figure 8, the range of crisp HOM is [0, 5] in units of dB. Moreover, Figure 9 illustrates that the range of crisp TTT is [0, 200] in terms of milliseconds.

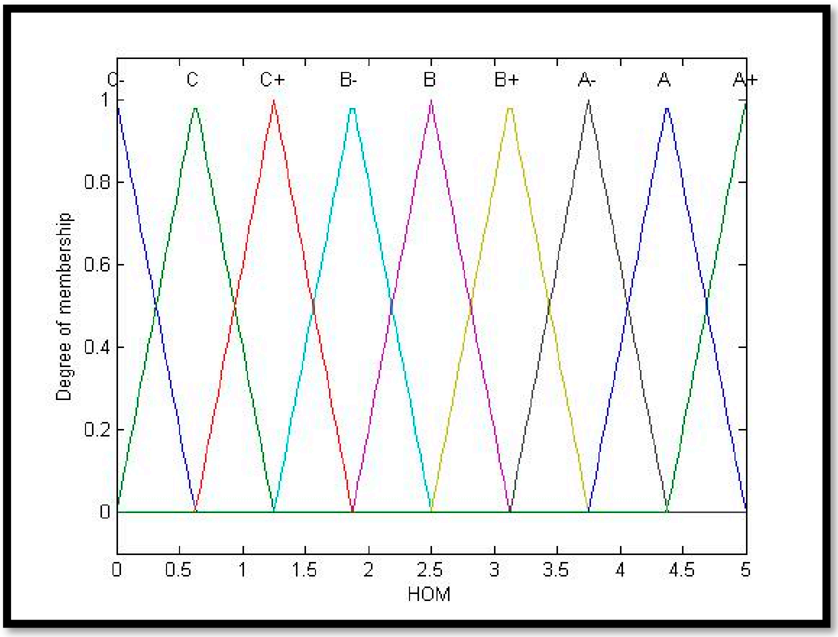

Figure 8. Membership function of linguistic HOM.

3.2.3. Handover Decision

In the handover decision stage, the HOM and TTT values obtained from the preceding stage are used to make the handover decision. In addition to dynamically adjusting the HOM and TTT, only the neighboring BSs that make an angle of less than ±90° with the moving direction of the UE are target BS candidates. This condition ensures that only the BSs in front of the UE can be the target BS candidates to have a more accurate selection of the target BS within a relatively short time. The pseudocode of the handover decision procedure is presented in Table 4. The UE periodically sends its measurement reports, and all calculations are performed at the serving BS. When the SINR with respect to a certain neighboring BS is greater than the SINR of the serving BS plus HOM for a duration of TTT and the angle between the UE moving direction and the neighboring BS is less than $\pm 90^{\circ}$, handover from the serving BS to the neighboring BS is performed. If multiple candidate BSs simultaneously arrive at the handover decision, the BS with the largest SINR is selected as the handover target.

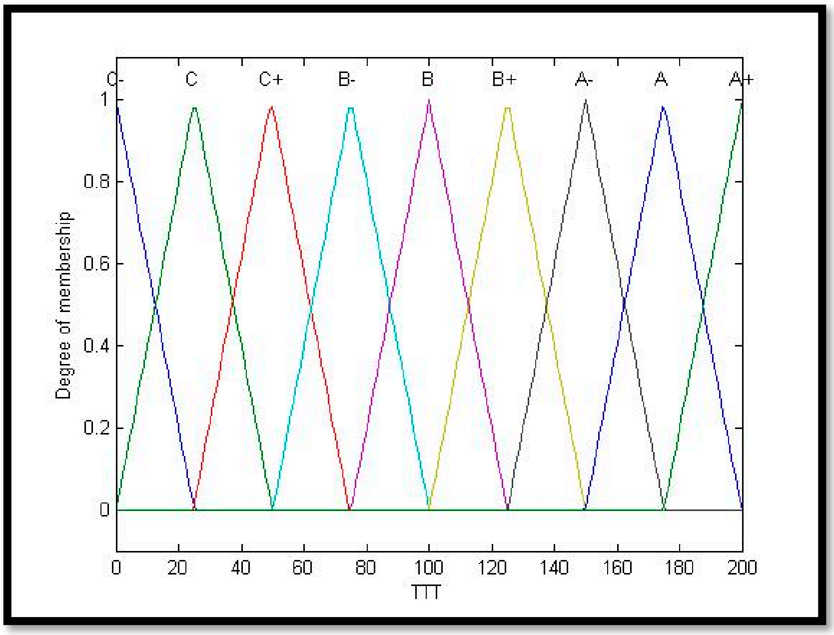

Figure 9. Membership function of linguistic TTT.

Table 4. Pseudocode of handover decision.

Input: $SINR_{serving}$, $SINR_{neighbor}$[M], HOM, TTT, $\cos\theta_{UEtoBS[i]}$
Output: Target BS of handover//return 0, in case of no handover execution
SINR_MAX = 0
Timer = 0;
Target = 0;
for i = 1:M **do**
while ($\cos\theta_{UEtoBS}[i] > 0$ && $SINR_{neighbor}[i] > SINR_{serving}$ + HOM && Timer < TTT)
    Timer++
if ($SINR_{neighbor}[i] \leqq SINR_{source}$ + HOM) **then**
    break
if (Timer==TTT && $SINR_{neighbor}[i]$ > SINR_MAX) **then**
SINR_MAX = $SINR_{neighbor}[i]$
Target = i
end for
return Target;

4. Performance Evaluation

To demonstrate the superiority and effectiveness of FLDHDT for 5G UDNs, simulations were performed on ns-3 [30] by using the conventional Event A3, FLDH [20], and FLDHDT handover schemes. The performance measures included the number of handovers, overall system throughput, and ping-pong ratio.

4.1. Simulation Settings

The 5G UDN topology used for performance evaluation is illustrated in Figure 10, and it is created by referring to the set up used in [20]. As elaborated in Section 3.1, Option 3 of the NSA networking mode was used. In an area measuring 300 m^2, three eNBs (blue circle dots) with fixed positions were deployed. Five, ten, and fifteen randomly distributed gNBs (red circle dots) were deployed. All the BSs communicate with each other through the X2 interface. Each eNB is connected to the EPC through S1-MME. Five UEs were randomly positioned in the simulation area with a two-dimensional random-walk mobility model [31]. The speed of each UE varied from 2 to 20 m/s. The simulation duration was 30 s. The other parameters and their values in the simulation are summarized in Table 5.

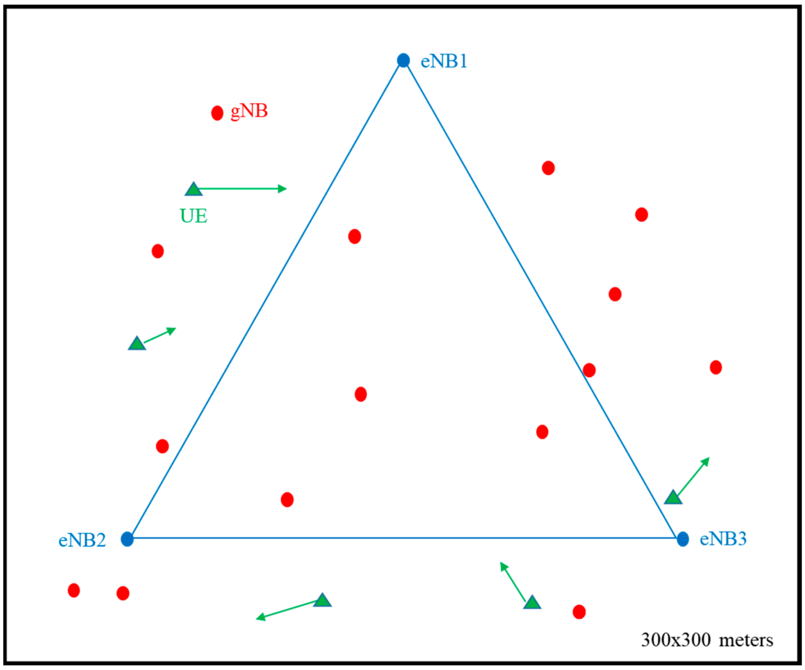

Figure 10. 5G UDN topology used in the simulation.

Table 5. Simulation parameter settings.

Parameters	Values
Simulator	NS3-3.30
Simulation area	300 × 300 m
Number of eNBs	3
Number of gNBs	5, 10, 15
Number of UEs	5
UE mobility model	2-D random walk
UE speed	2~20 m/s
Power of eNB/gNB	43 dBm/23 dBm
Frequency of eNB/gNB	2.4 GHz/28 GHz
Packet inter-arrival time	20 microseconds
Packet size	1000 bytes
Measurement report period	200 milliseconds
eNB Bandwidth	20 Mbps
gNB Bandwidth	100 Mbps
Simulation time	30 s

4.2. Results and Discussions

The performance of FLDHDT is compared with Event A3 and FLDH [14], and Table 6 summarizes the differences among the three schemes. All results are averages obtained over 10 simulation runs. The performance measures are the number of handovers, overall system throughput, and ping-pong ratio.

Table 6. Differences among event A3, FLDH, and FLDHDT.

Scheme	Event A3	FLDH	FLDHDT
Using fuzzy logic	No	Yes	Yes
HOM	fixed	dynamic	dynamic
TTT	fixed	fixed	dynamic

Figure 11 shows a plot of the number of handovers versus the number of gNBs with the Event A3, FLDH, and FLDHDT schemes. Among the three schemes, Event A3 had the largest number of handovers because, in making the handover decision, the Event A3 scheme considers only the signal strength of the UE. Furthermore, FLDH can dynamically adjust the HOM such that a UE with a higher signal strength has a higher HOM to avoid unnecessary handovers. As for FLDHDT, it had the smallest number of handovers because both HOM and TTT are dynamically adjusted based on the signal strength and horizontal speed of the UE. Moreover, it is apparent that the number of handovers for any of the three schemes increases with the number of gNBs due to the increase in small BS density.

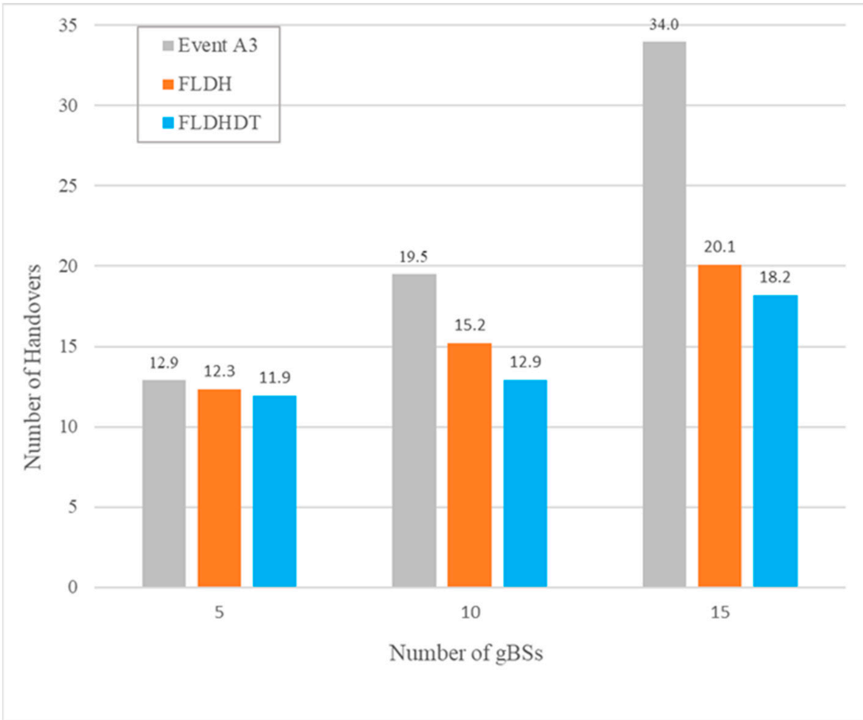

Figure 11. Number of handovers versus number of gNBs.

A ping-pong handover is defined as occurring when a device changes connection from BS A to BS B and switches back to BS A within 1 s. The ping-pong ratio, denoted R_{pp}, is the number of ping-pong handovers divided by the total number of handovers, as expressed in Equation (4). According to Figure 12, the ping-pong ratio invariably increases as the density of small BSs increases, but FLDHDT improves Rpp compared to the two other schemes, especially in dense UDNs. However, dynamic HOM causes a more significant improvement than dynamic TTT, and the difference between the ping-pong ratios of FLDHDT and FLDH for 15 gNBs is marginally smaller than for 10 gNBs. This is because HOM is essentially the most important parameter when making handover decision.

$$R_{pp} = \frac{\text{no. of ping} - \text{pong handovers}}{\text{total no. of handovers}} \times 100\% \quad (4)$$

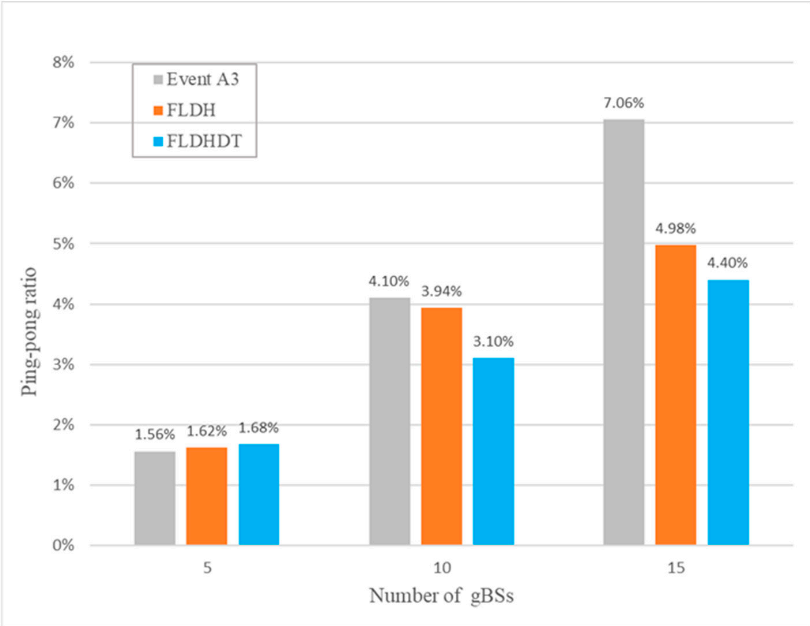

Figure 12. Ping-pong ratio versus number of gNBs.

As depicted in Figure 13, the overall system throughput is improved by FLDH or FLDHDT for dense UDNs because these schemes reduce the number of handovers by using dynamic HOM or TTT. Notably, shortening the TTT can reduce the interruption gap due to hard handover and alleviate packet loss to improve the throughput of each UE. Therefore, the higher the density of small BSs is, the more substantial is the improvement due to FLDHDT compared to Event A3 and FLDH.

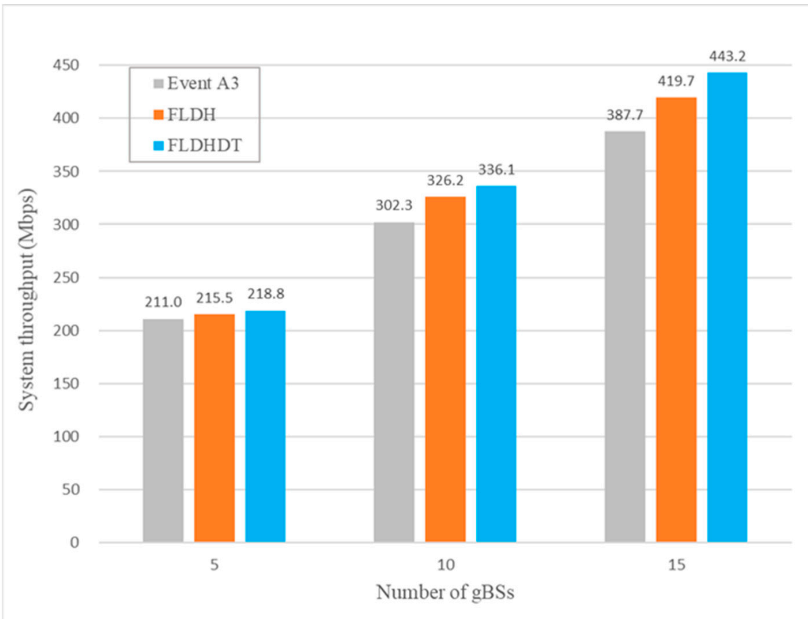

Figure 13. System throughput versus number of gNBs.

5. Conclusions

In this study, we have proposed an FL-based handover scheme for 5G UDNs. The proposed scheme can dynamically adjust two handover parameters, namely HOM and TTT, by using the SINR and horizontal moving speed of UE as inputs to an FL controller. The proposed scheme is designated FLDHDT. Similar to other handover decision schemes, signal strength is considered an important factor when making handover decision in FLDHDT. A higher signal strength inevitably leads to a higher HOM. Moreover, UE velocity is an input factor governing handover decision in FLDHDT. A higher UE speed warrants a shorter TTT. The proposed FLDHDT reduces the number of unnecessary handovers and shortens the interruption gap caused by hard handovers. Moreover, only the BSs in front of the UE can be the target BS candidates to ensure more accurate selection of target BS within a relatively short time. The superiority of FLDHDT has been verified by conducting a simulation in which it substantially improved the handover performance of 5G UDNs in terms of the number of handovers, ping-pong ratio, and overall system throughput compared to a conventional handover scheme, namely Event A3, and an FL-based handover scheme with dynamic adjustment of only HOM. In the future, we intend to design a more practical FL-based handover scheme by considering different coverages of small BSs and providing additional inputs to the FL controller, such as BS loading.

Author Contributions: Conceptualization, W.-S.H. and Y.-J.W.; methodology, W.-S.H., Y.-J.W. and M.-H.C.; software, T.-Y.C. and M.-H.C.; validation, T.-Y.C. and M.-H.C.; formal analysis, T.-Y.C.; investigation, T.-Y.C. and M.-H.C.; data curation, T.-Y.C.; writing—original draft preparation, W.-S.H.; writing—review and editing, Y.-J.W.; visualization, T.-Y.C. and M.-H.C.; supervision, W.-S.H.; project administration, W.-S.H.; funding acquisition, W.-S.H. All authors have read and agreed to the published version of the manuscript.

Funding: This research was supported in part by Taiwan Ministry of Science and Technology under Grant No.: MOST 110-2221-E-992-029-MY2. And, the APC was supported in part by Shih Chien University Research Project with the Grant No.: USC-111-08-01008.

Data Availability Statement: The data used to support the findings of this study are available from the corresponding author upon request.

Acknowledgments: We thank the anonymous reviewers for their constructive comments, which helped in improving the quality of this paper.

Conflicts of Interest: The authors declare no conflict of interest.

References

1. Network Experience Evolution to 5G. Available online: https://www.gsma.com/futurenetworks/resources/network-experience-evolution-to-5g/ (accessed on 1 September 2022).
2. Mobile Data Traffic Outlook. Available online: https://www.ericsson.com/en/reports-and-papers/mobility-report/dataforecasts/mobile-traffic-forecast (accessed on 1 September 2022).
3. Lin, Z.; Niu, H.; An, K.; Wang, Y.; Zheng, G.; Chatzinotas, S.; Hu, Y. Refracting RIS-Aided Hybrid Satellite-Terrestrial Relay Networks: Joint Beamforming Design and Optimization. *IEEE Trans. Aerosp. Electron. Syst.* **2022**, *58*, 3717–3724. [CrossRef]
4. Lin, Z.; An, K.; Niu, H.; Hu, Y.; Chatzinotas, S.; Zheng, G.; Wang, J. SLNR-based Secure Energy Efficient Beamforming in Multibeam Satellite Systems. *IEEE Trans. Aerosp. Electron. Syst.* **2022**. [CrossRef]
5. Lin, Z.; Lin, M.; Wang, J.B.; De Cola, T.; Wang, J. Joint Beamforming and Power Allocation for Satellite-Terrestrial Integrated Networks with Non-Orthogonal Multiple Access. *IEEE J. Sel. Top. Signal Process.* **2019**, *13*, 657–670. [CrossRef]
6. Park, J.; Kim, S.-L.; Zander, J. Asymptotic Behavior of Ultra-Dense Cellular Networks and Its Economic Impact. In Proceedings of the 2014 IEEE Global Communications Conference, Austin, TX, USA, 8–12 December 2014; pp. 4941–4946.
7. Su, L.; Yang, C.; Chih-Lin, I. Energy and Spectral Efficient Frequency Reuse of Ultra Dense Networks. *IEEE Trans. Wirel. Commun.* **2016**, *15*, 5384–5398. [CrossRef]
8. Baldemair, R.; Irnich, T.; Balachandran, K.; Dahlman, E.; Mildh, G.; Selén, Y.; Parkvall, S.; Meyer, M.; Osseiran, A. Ultra-Dense Networks in Millimeter-Wave Frequencies. *IEEE Commun. Mag.* **2015**, *53*, 202–208. [CrossRef]
9. Liu, J.; Xiao, W.; Soong, A.C.; Anpalagan, A.; Bennis, M.; Vannithamby, R. Dense Networks of Small Cells. In *Design and Deployment of Small Cell Networks*; Cambridge University Press: Cambridge, UK, 2015; pp. 96–121.
10. 5G; NR; Radio Resource Control (RRC); Protocol Specification (3GPP TS 38.331 Version 15.3.0 Release 15). Available online: https://www.etsi.org/deliver/etsi_ts/138300_138399/138331/15.03.00_60/ts_138331v150300p.pdf (accessed on 1 September 2022).

11. Zadeh, L.A. Fuzzy Sets. *Inf. Control* **1965**, *8*, 338–353. [CrossRef]
12. Bansod, N.A.; Kulkarni, M.; Patil, S.H. Soft Computing—A Fuzzy Logic Approach. In *Soft Computing*; Allied Publishers: New Delhi, India, 2005; pp. 73–75.
13. Kaur, K.; Goyal, S.; Bhullar, A.K. Handover for 5G Networks using Fuzzy Logic: A Review. *Int. J. Electr. Electron. Comput.* **2021**, *6*, 25–33. [CrossRef]
14. Duo, R.; Wu, C.; Yoshinaga, T.; Zhang, J.; Ji, Y. SDN-based Handover Scheme in Cellular/IEEE 802.11p Hybrid Vehicular Networks. *Sensors* **2020**, *20*, 1082. [CrossRef] [PubMed]
15. Lee, J.; Yoo, Y. Handover cell Selection Using User Mobility Information in a 5G SDN-based Network. In Proceedings of the 2017 9th International Conference on Ubiquitous and Future Networks (ICUFN), Milan, Italy, 4–7 July 2017; pp. 697–702.
16. Mollel, M.S.; Abubakar, A.I.; Ozturk, M.; Kaijage, S.F.; Kisangiri, M.; Hussain, S.; Imran, M.A.; Abbasi, Q.H. A Survey of Machine Learning Applications to Handover Management in 5G and Beyond. *IEEE Access* **2021**, *9*, 45770–45802. [CrossRef]
17. Tanveer, J.; Haider, A.; Ali, R.; Kim, A. An Overview of Reinforcement Learning Algorithms for Handover Management in 5G Ultra-Dense Small Cell Networks. *Appl. Sci.* **2022**, *12*, 426. [CrossRef]
18. Yajnanarayana, V.; Rydén, H.; Hévizi, L. 5G Handover Using Reinforcement Learning. In Proceedings of the 2020 IEEE 3rd 5G World Forum (5GWF), Bangalore, India, 10–12 September 2020; pp. 349–354.
19. Zhao, S.; Jiang, X.; Jacobson, G.; Jana, R.; Hsu, W.L.; Rustamov, R.; Talasila, M.; Aftab, S.A.; Chen, Y.; Borcea, C. Cellular Network Traffic Prediction Incorporating Handover: A Graph Convolutional Approach. In Proceedings of the 2020 17th Annual IEEE International Conference on Sensing, Communication, and Networking (SECON), Como, Italy, 22–25 June 2020; pp. 1–9.
20. Chen, Y.S.; Chang, Y.J.; Tsai, M.J.; Sheu, J.P. Fuzzy-Logic-Based Handover Algorithm for 5G Networks. In Proceedings of the 2021 IEEE Wireless Communications and Networking Conference (WCNC), Nanjing, China, 29 March–1 April 2021; pp. 1–7.
21. Souza, D.D.S.; Vieira, R.F.; Seruffo, M.-H.C.D.R.; Cardoso, D.L. A Novel Heuristic for Handover Priority in Mobile Heterogeneous Networks. *IEEE Access* **2019**, *8*, 4043–4050. [CrossRef]
22. Goutam, S.; Unnikrishnan, S.; Singh, P.; Karandikar, A. Algorithm for Handover Decision Using Fuzzy Logic. In Proceedings of the 2020 IEEE Bombay Section Signature Conference (IBSSC), Mumbai, India, 4–6 December 2020; pp. 25–30.
23. Huey, R.-S.; Lin, T.-M.; Hsu, C.-K. Predictive Handover Approach for Dynamic Resource Management in 5G Heterogeneous Networks using Grey Fuzzy Logical Control. In Proceedings of the 2022 8th International Conference on Applied System Innovation (ICASI), Nantou, Taiwan, 22–23 April 2022; pp. 187–192.
24. Banna, R.E.; ELAttar, H.M.; Abou El-Dahab, M.M. Fast Adaptive Handover using Fuzzy Logic for 5G Communications on High Speed Trains. In Proceedings of the 2021 16th International Conference on Telecommunications (ConTEL), Zagreb, Croatia, 30 June–2 July 2021; pp. 10–17.
25. Alraih, S.; Nordin, R.; Abu-Samah, A.; Shayea, I.; Abdullah, N.F.; Alhammadi, A. Robust Handover Optimization Technique with Fuzzy Logic Controller for Beyond 5G Mobile Networks. *Sensors* **2022**, *22*, 6199. [CrossRef]
26. Mamdani, E.H.; Assilian, S. An Experiment in Linguistic Synthesis with a Fuzzy Logic Controller. *Int. J. Man-Mach. Stud.* **1975**, *7*, 1–13. [CrossRef]
27. Hájek, P. *Metamathematics of Fuzzy Logic*; Kluwer Academic Publishers: Dordrecht, The Netherlands; Boston, MA, USA; London, UK, 1998.
28. LTE Metrics Including RSRP, RSRQ and SINR. Available online: https://www.cablefree.net/wirelesstechnology/4glte/lte-rsrq-sinr/ (accessed on 1 September 2022).
29. Abbas, A. Fuzzy Logic Control in Support of Autonomous Navigation of Humanitarian De-mining Robots. In *Book Chapter of Using Robots in Hazardous Environments*; Elsevier: Amsterdam, The Netherlands, 2011; pp. 453–475.
30. ns-3 Simulator with mmWave Module. Available online: https://github.com/nyuwireless-unipd/ns3-mmwave (accessed on 1 September 2022).
31. Chiang, K.-H.; Shenoy, N. A 2-D Random-Walk Mobility Model for Location-Management Studies in Wireless Networks. *IEEE Trans. Veh. Technol.* **2004**, *53*, 413–424. [CrossRef]